Three-Dimensional Printing in Catalysis: Combining 3D Heterogeneous Copper and Palladium Catalysts for Multicatalytic Multicomponent Reactions

Antonio S. Díaz-Marta,[1,‡] Carmen R. Tubío,[2,‡] Carlos Carbajales,[1] Carmen Fernández,[1] Luz Escalante,[1] Eddy Sotelo,[1,4] Francisco Guitián,[2] V. Laura Barrio,[3] Alvaro Gil*[,2] and Alberto Coelho*[,1,4]

[1]Centro Singular de Investigación en Química Biolóxica e Materiáis Moleculares (CIQUS), Universidade de Santiago de Compostela, 15782, Spain

[2]Instituto de Cerámica, Universidade de Santiago de Compostela, 15782, Santiago de Compostela, Spain

[3]Escuela de Ingeniería. Universidad del País Vasco, Alameda Urquijo s/n, 48013, Bilbao, Spain

[4]Departamento de Química Orgánica, Facultad de Farmacia. Universidade de Santiago de Compostela, 15782, Santiago de Compostela, Spain

ABSTRACT: Two 3D-hybrid monolithic catalysts containing immobilized copper and palladium species on a silica support were synthesized by 3D printing and a subsequent surface functionalization protocol. The resulting 3D monoliths provided a structure with high mechanical strength, controlled porosity, and easy catalyst recyclability. The devices were designed to perform heterogeneous Multicatalytic Multicomponent Reactions (MMCRs) based on a Copper Alkyne-Azide Cycloaddition (CuAAC) + Palladium Catalyzed Cross-Coupling (PCCC) strategy, which allowed the rapid assembly of variously substituted 1,2,3-triazoles using a mixture of tBuOH/H_2O as solvents. The reusable multicatalytic system developed in this work is an example of a practical miniaturized and compartmental heterogeneous 3D-printed metal catalyst to perform MMCRs for solution chemistry.

KEYWORDS: 3D-Printing, Heterogeneous catalysts, CuAAC, Palladium, Multicatalytic Multicomponent reactions.

INTRODUCTION

The application of efficient catalytic processes instead of stoichiometric ones is one of the main requirements for sustainable and environmentally friendly chemistry.[1] Among the known catalytic transformations, Transition Metal-Catalyzed Reactions (TMCRs)[2] form one of the main pillars of Modern Organic Chemistry and they are of great importance for applications in the chemical, pharmaceutical, and biochemical industries. However, the use of homogeneous TMCRs on an industrial scale suffers from serious drawbacks that concern the final product.[3] For instance, the synthesis of active pharmaceutical ingredients in the pharmaceutical industry is subject to strict safety regulations and trials to determine the presence of traces of metals in the final products.[4] Therefore, immobilizing catalytic metal species on solid reusable supports for an easier catalyst separation and reuse while avoiding leaching processes is currently a key priority to develop cleaner and more sustainable chemistry. Attempts to increase the flexibility of heterogeneous solid catalysts have been made by synthesizing hybrid organic–inorganic structured solids that contain active sites in either one or both components. Such solids include hybrid zeolites,[5] periodic mesoporous organosilicas (PMOs),[6] metal–organic frameworks (MOFs),[7,8] and, in general, hybrid organic–inorganic catalysts.[9]

The overall objective for truly sustainable chemistry is not only achievable through the discovery of new recoverable solid heterogeneous catalysts based on novel materials, but also through the synergistic application of these devices in modular, robust and efficient chemical transformations. In 2001, Sharpless, Finn, and Kolb laid out the philosophy of click chemistry,[10] an innovative approach to chemical synthesis. The prototypical click chemistry reaction, the copper catalyzed azide-alkyne cycloaddition (CuAAC),[11] was independently reported by Sharpless[12] and Meldal,[13] who described the dramatic improvement of the original Huisgen process through the use of a copper(I) catalyst. Another paradigm of chemical efficiency is represented by the palladium-catalyzed cross-coupling reactions (PCCCR).[14] In terms of industrial applications, Suzuki coupling is by far the most widely used reaction of this type, followed by Heck, Sonogashira and Stille couplings. Despite the impact of CuAAC and PCCCRs, and given the drawbacks related to their application under homogeneous conditions on an industrial scale as discussed above, efforts to carry out these transformations under heterogeneous conditions have attracted the attention of chemists in the last two decades.[15]

On considering the use of efficient transformations, the multicomponent reactions (MCRs)[16,17] are particularly powerful chemical methodologies. These reactions are characterized by their convergence, atom economy, and the avoidance of intermediate purification processes. As a consequence, these reactions have considerable advantages over classical linear syntheses. Although most of the established MCRs do not require a catalyst, the search for new MCR products has resulted in great effort to find catalysts and new catalyzed MCRs.[18] Consequently, (MMCRs)[19] have emerged as a highly valuable synthetic tool. In an MMCR, two or more catalysts are present from the onset of the reaction and these operate independently and in a consecutive manner. Cooperative catalysis provided by copper and palladium sources has been explored[20,21] in an exhilarating and fruitful manner as well as rhodium/palladium,[22] rhodium/palladium/copper,[23] indium/palladium,[24] copper/rhodium[25] and rhodium/iridium[26] combinations, although in these procedures the pairs were always used as homogeneous catalysts. Despite the impressive

possibilities provided by the combination of heterogeneous metal catalysts in different multicomponent cocktails, to our knowledge, examples of compartmentalized bulky 3D monolithic heterogeneous catalytic systems in MMCRs have not been reported (at least two catalysts in the reaction mixture). The use of monolithic catalysts in catalytic processes offers significant advantages compared to traditional catalytic materials such as powders, pellets and extrudates, thus offering an easier handling and a better reusability. A powerful argument for the use of 3D monoliths in catalysis is related to the individual recovery and recycling after an MMCR or tandem process. For example, on using the traditional catalytic systems cited above, the complexity of performing a powder solid-solid separation during work up (only achievable by the incorporation of magnetic properties[27,28] on supports or the use of the *Houghten 'Tea bag'* method[29]) can be solved by the simple compartmentalization of immobilized active catalytic metal species within 3D monolithic structures. 3D Monolithic catalysts also have numerous advantages over packed-bed reactors and these include high transport rates of heat and mass per unit pressure drop, small transverse temperature gradients, and ease of scale up.[30]

Shape and size are key aspects in the design of heterogeneous catalysts[31] and 3D printing offers the possibility of modulating of these macroscopic aspects for catalysts. This revolutionary technology stands out due to the key advantage of the fabrication of three-dimensional physical objects from a digital model by taking a virtual design from computer-aided design (CAD) software and reproducing it layer by layer until the physical definition of the layers gives the designed product.[32] The 3D printing technique enables the fabrication of monoliths with different cross sections, pore sizes, and wall thicknesses, thus maximizing the catalytic surface. More importantly, the fabrication parameters can be tuned to obtain parts with excellent mechanical properties. A wide range of 3D printing materials can produce tough functional prototypes for highly accurate performance testing, or realistic models that look and feel like the finished products. Therefore, 3D printing provides knowledge on exactly how a 3D-catalyst will look and perform before investing in tooling.

In recent years, 3D-printed monoliths based on doped polymers, carbon materials, metal and metal oxides, or zeolites have received considerable attention for use in adsorption systems as well as 3D-printed inorganic monoliths for single catalytic transformations.[33] A combination of 3D printing and surface modification was recently explored by directly integrating a Br-containing vinyl-terminated initiator into the 3D resin followed by surface-initiated atomic-transfer radical polymerization (ATRP) and subsequent electroless plating in a process that enables the formation of complex metallic architectures.[34] The development of catalysts based on ceramic materials is a great challenge for 3D printing technology. Recently, our group reported the first 3D printed heterogeneous copper catalyst on an alumina support (obtained by a copper/Al_2O_3-based ink extrusion and subsequent sintering to obtain a CuO surface) and its application in Ullmann reactions.[35] We later proposed the fabrication of hybrid (inorganic support/organic functionality on the surface) heterogeneous 3D printed monolithic catalysts obtained by chemical surface modification and their application in new MMCRs.

Silica-based surfaces show both excellent mechanical stability and reactivity against silanization compared to other oxides (Al_2O_3, clays, silicon, TiO_2, SnO, Fe_2O_3, etc.). Silanization allows the functionalization of the monolithic surface and the attachment of appropriate linkers containing coordination sites for catalytic metal species.[36] In this work, we carried out the synthesis of two new silica-based Pd and Cu heterogeneous monolithic catalysts [3D-SiO_2-APTS-Cu and 3D-SiO_2-AAPTS-Pd] by 3D printing of a silica support followed by surface functionalization and we evaluated the catalytic activity of these materials in newly designed CuAAC + Sonogashira, CuAAC + Stille or CuAAC + Suzuki MMCRs. The experimental protocol was performed in six stages: (1) Preparation of concentrated colloidal gel ink in which SiO_2 ceramic powder and polymer binders were mixed to obtain a good homogeneity. (2) Extrusion to build a 3D woodpile structure. (3) Sintering of the structure at high temperature. (4) Surface activation in acid media and subsequent functionalization by silanization and metallation to give the final 3D-monolithic copper (3D-SiO_2-APTS-Cu) and palladium (3D-SiO_2-AAPTS-Pd) structures. (5) Validation of the catalytic efficacy in Cu-AAC, Sonogashira, Stille and Suzuki reactions and finally (6) Evaluation of the combined use of both catalytic systems in MMCRs.

EXPERIMENTAL SECTION

3D printed SiO_2 monolith fabrication. The SiO_2 colloidal ink was prepared as described previously[37] by mixing 50 g of SiO_2 powder (average particle size 6.3 μm), 12.08 g of poly(vinyl butyral-co-vinyl alcohol-co-vinyl acetate) (PVB-PVA-PVAc, 80 wt% vinyl butyral) and 3.99 g of polyethylene glycol (PEG, Mw = 600) in 32.55 mL of 2-propanol (≥ 99.5%). All reagents were obtained from Sigma-Aldrich. The ink was mixed in a planetary centrifugal mixer (ARE-250, Thinky Corp., Tokyo Japan) at 2000 rpm for 5 cycles of 2 min. The ink was transferred into a 3 mL syringe barrel (Nordson EFD, USA) fitted to a cylindrical nozzle (diameter of 410 μm, EFD). An air pressure system (Performus VII with HP7x, EFD) was attached to the syringe barrel to provide the required pressure to extrude the ink through the nozzle. The structures were printed using a robotic deposition apparatus (Model A3200, Aerotech Inc., USA). The resulting catalysts consisted of cylinder structures of 40 layers and 10 mm diameter with a body-centered tetragonal (bct) symmetry, a rod diameter of 410 μm and rod spacing of 1 mm. After fabrication and drying, the samples were debinded at 400 °C for 1 h at a heating rate of 2 ºC/min and subsequently sintered at 1500 °C for 3 h at a heating rate of 5 ºC/min.

Surface activation. A SiO_2-monolith (1.3 cm in height × 0.8 cm diameter) was submerged in a solution of H_2O_2 (30%) and heated under reflux at 150 ºC for 30 min. The monolith was removed from the flask and treated with distilled water at 100 ºC for 30 min. After this treatment, the monolith was dried under vacuum for 1 h. Kimble® vials in a PLS (6 × 4) Organic Synthesizer were used to perform the surface functionalization of the SiO_2-monoliths and the CuAAC, PCCCRs, and MMCRs.

Silanization. Silanization for the synthesis of the 3D-SiO_2-APTS-Cu catalyst: in a Kimble vial, an activated 3D-monolith was submerged in a solution of (3-aminopropyl)trimethoxysilane (APTS) (0.5 mL) in dry toluene (8 mL). The mixture was heated at 120 ºC for 24 h under argon. The monolith was filtered off, washed with toluene and ethanol and dried under vacuum for 24 h. The same conditions as before, but using [3-(2-aminoethylamino)-propyl]trimethoxysilane (AAPTS) as the reagent, were used for silanization prior to the synthesis of the 3D-SiO_2-AAPTS-Pd catalyst.

Metallation. The 3D-SiO_2-APTS monolith obtained in the previous step was treated with a solution of CuI (10 mg) in 8 mL of acetonitrile (MeCN) at 40 °C with orbital stirring during 12 h to obtain 3D-SiO_2-APTS-Cu. Similarly, the 3D-SiO_2-AAPTS monolith was reacted with a solution of $Pd(AcO)_2$ (15 mg) in 8 mL of anhydrous N,N-dimethylformamide (DMF) at 60 ºC with orbital stirring overnight to give the 3D-SiO_2-AAPTS-Pd catalyst. The resulting colored monolithic catalysts were washed and sonicated with distilled water, methanol (MeOH), dichloromethane (CH_2Cl_2), and diethyl ether, and finally dried under reduced pressure for 24 h.

Catalyst characterization. The microstructural surface morphology of the 3D printed SiO_2 catalysts were examined by scanning electron microscopy (SEM) (JEOL 6400, JEOL Corp., Japan). Optical microscopy images were obtained on an Olympus SZX12 stereomicroscope (Olympus, Japan). Specific surface area measurements of the 3D printed monoliths were performed according to the Brunauer–Emmett–Teller (BET) nitrogen adsorption method at 77 K in a Gemini 2360 porosimeter (Micrometitics, USA). All samples were degassed at 300 ºC for 2 h before the BET analysis. The chemical composition of the catalysts was evaluated by energy dispersive X-ray spectrometry (AZTEC/Xact, Oxford, UK). The copper and palladium loadings of the structures were determined by inductively coupled plasma-optical emission spectroscopy (ICP-OES, Varian Liberty 200). The oxidation states of Cu and Pd were determined by X-ray photoelectron spectroscopy (XPS) using a Thermo Scientific K-Alpha ESCA instrument equipped with aluminum Kα monochromatized radiation at 1486.6 eV as the X-ray source. Due to the non-conducting nature of the samples it was necessary to use an electron flood gun to minimize surface charging. Neutralization of the surface charge was performed by using both a low energy flood gun (electrons in the range 0 to 14 eV) and a low energy Argon ion gun. The XPS measurements were carried out using monochromatic Al-Kα (1486.6 eV) X-ray radiation. Photoelectrons were collected from a take-off angle of 90º relative to the sample surface. The measurement was carried out in Constant Analyzer Energy mode (CAE) with a 100 eV pass energy for survey spectra and 20 eV pass energy for high resolution spectra. Time of Flight Secondary Ions Mass Spectrometry (TOF-SIMS) was used to record the 2D chemical MAPS of the 3D-SiO_2-APTS-Cu and 3D-SiO_2-AAPTS-Pd catalyst surfaces. TOF-SIMS measurements were performed with an ION-TOF GmbH instrument (TOF-SIMS 4) using a 25 keV pulsed $^{208}Bi^{3+}$ primary analysis Ion Gun and a raster size of 500×500 μm^2 producing a sample current of 0.37 pA.

Evaluation of the catalytic activity. All reactions were monitored by TLC with 2.5 mm Merck silica gel GF 254 strips and the purified compounds showed a single spot. Detection of compounds was performed by UV light and/or iodine vapor. Purification of isolated products was carried out by flash chromatography with an ISCO Combiflash system that employs prepacked silica gel columns. The synthesized compounds were characterized by spectroscopic and analytical data. The NMR spectra were recorded on Bruker AM 300 MHz (^1H) and 75 MHz (^{13}C) and XM500 spectrometers. Chemical shifts are given as δ values against tetramethylsilane as internal standard and *J* values are given in Hz. Proton and carbon nuclear magnetic resonance spectra (^1H, ^{13}C NMR) were recorded in $CDCl_3$. Melting points were determined on a Gallenkamp melting point apparatus and are uncorrected. Mass spectra were obtained on a Varian MAT-711 instrument. High resolution mass spectra (HR-MS) were obtained on an Autospec Micromass spectrometer.

Synthesis of compound 1 by CuAAC. In a coated Kimble vial were dissolved sodium azide (0.5 mmol), 2-iodobenzyl bromide (0.5 mmol), DIPEA (1.5 mmol) and phenylacetylene (0.5 mmol), in a mixture of tBuOH (3 mL)/H_2O (1 mL). To this solution was added the 3D-SiO_2-APTS-Cu catalyst (total Cu content on the monolith: 0.6 mg). The mixture was orbitally stirred for 12 h at room temperature. The white solid formed in the vessel was dissolved in AcOEt. The monolithic catalyst 3D-SiO_2-APTS-Cu was then removed from the solution, washed and sonicated with EtOH/CH_2Cl_2/H_2O and dried under vacuum for reuse. The resulting solution was washed with H_2O. The organic phase was extracted with AcOEt and dried with anhydrous Na_2SO_4. The solvent was removed under reduced pressure and the resulting solid was recrystallized (iPrOH) to give compound **1** as a light white solid.

Synthesis of compound 2 by Sonogashira reaction. In a coated Kimble vial the iodotriazole **1** (0.5 mmol), DIPEA (1.5 mmol) and phenylacetylene (0.6 mmol) were dissolved in a mixture of tBuOH (3 mL)/H_2O (1 mL). To this solution was added the 3D-SiO_2-AAPTS-Pd monolithic catalyst (total Pd content on monolith: 1.6 mg). The mixture was heated with orbital stirring at 100 °C for 6 h until the starting material had been consumed. The mixture was allowed to cool and the catalyst was removed, washed and sonicated with EtOH/CH_2Cl_2/H_2O for reuse. The mixture was washed with H_2O. The organic phase was extracted with AcOEt and dried with anhydrous Na_2SO_4. The solvent was removed under reduced pressure and the resulting solid was purified by flash cromatography (AcOEt/Hexane,1:4) and recrystallized (iPrOH) to give compound **2** as a light white solid.

Synthesis of compound 14 by Stille reaction. In a coated Kimble vial, the iodotriazole **1** (0.5 mmol) and the corresponding organostannane (0.6 mmol) were dissolved in a mixture of tBuOH (3 mL)/H_2O (1 mL). To this solution was added the 3D-SiO_2-AAPTS-Pd catalyst (total Pd content on monolith: 1.6 mg). The mixture was heated at 80 °C with orbital stirring for 2 h until the starting material had been consumed. The mixture was allowed to cool and the catalyst was extracted from the vial, washed and recovered for reuse. The mixture was washed with a solution of KF (1M, 3 × 10 mL) for removing tin byproducts. The organic phase was extracted with AcOEt and dried with anhydrous Na_2SO_4. The solvent was removed under reduced pressure and the solid was purified by flash cromatography (DCM/MeOH) and recrystallization (iPrOH) to give compound **14** as a light yellow solid.

Synthesis of compound 20 by Suzuki reaction. In a coated Kimble vial the iodotriazole **1** (0.5 mmol), DIPEA (2.5 mmol) and the corresponding boronic acid (0.6 mmol) were dissolved in a mixture of tBuOH (3 mL)/H_2O (1 mL). To this solution was added the 3D-SiO_2-AAPTS-Pd catalyst (total Pd content on monolith: 1.6 mg). The mixture was heated at 90 °C for 2 h until the starting material had been consumed. The mixture was allowed to cool and the catalyst was removed, washed and sonicated with EtOH/CH_2Cl_2/H_2O for reuse. The mixture was washed with H_2O. The organic phase was extracted with AcOEt and dried with anhydrous Na_2SO_4. The solvent was removed under reduced pressure and the resulting solid was purified by recrystallization (iPrOH) to give compound **20** as a light white solid.

General procedure for CuAAC + Sonogashira MMCRs (synthesis of compounds 2–7). In a coated Kimble vial were dissolved sodium azide (0.5 mmol), the corresponding iodo-

benzyl bromide (0.5 mmol), DIPEA (1.5 mmol) and the alkyne (1.2 mmol) in a mixture of tBuOH (3 mL)/H_2O (1 mL). To this solution were added the 3D-SiO_2-APTS-Cu (total Cu content on monolith: 0.6 mg) and 3D-SiO_2-AAPTS-Pd (total Pd content on monolith: 1.6 mg) monolithic catalysts. The mixture was heated at 100 ºC for 12 h with orbital stirring. The solid formed on the vessel wall was dissolved in AcOEt. The monolithic catalysts were then removed from the solution, sonicated and washed with EtOH/CH_2Cl_2/H_2O and dried under vacuum for reuse. Final products were isolated by extraction with AcOEt/H_2O. The organic phase was dried with anhydrous Na_2SO_4, the solvent was removed under reduced pressure and the resulting product was purified by flash cromatography and recrystallization to give compounds **2-7**.

General procedure for the sequential one-pot CuAAC + Sonogashira MMCRs (3CR +1, synthesis of compounds 8–13). In a coated Kimble vial sodium azide (0.5 mmol), the corresponding iodobenzyl bromide (0.5 mmol), DIPEA (1.5 mmol) and the first alkyne (0.5 mmol) were dissolved in a mixture of tBuOH (3 mL)/H_2O (1 mL). To this solution were added the 3D-SiO_2-APTS-Cu (total Cu content on monolith: 0.6 mg) and 3D-SiO_2-AAPTS-Pd (total Pd content on monolith: 1.6 mg). The mixture was kept under orbital stirring for 12–16 hours at room temperature until the CuAAC reaction was complete (TLC). The corresponding second alkyne (0.6 mmol) was added and the mixture was heated at 100 ºC for 6 h until the corresponding iodo-intermediate had been consumed. The solid formed on the vessel wall was dissolved in AcOEt. The monolithic catalysts were then removed from the solution, sonicated and washed with EtOH/CH_2Cl_2/H_2O and dried under vacuum for reuse. Final products were isolated by extraction with AcOEt/H_2O. The organic phase was dried with anhydrous Na_2SO_4, the solvent was removed under reduced pressure and the resulting product was purified by flash cromatography and recrystallization to give compounds **8-13**.

General procedure for CuAAC + Stille MMCRs (synthesis of compounds 14–19). In a coated Kimble vial containing the 3D-SiO_2-APTS-Cu (overall Cu content on monolith: 0.6 mg) and 3D-SiO_2-AAPTS-Pd (overall Pd content on monolith: 1.6 mg) monolithic catalysts, sodium azide (0.5 mmol), the corresponding iodobenzyl bromide (0.5 mmol), DIPEA (1.5 mmol), the corresponding alkyne (0.5 mmol) and the organostannane (0.55 mmol) were dissolved in a mixture of tBuOH (3 mL)/H_2O (1 mL). The mixture was heated at 80 ºC for 12 h. The mixture was allowed to cool. The solid formed on the vessel wall was dissolved in AcOEt. The monolithic catalysts were then removed from the solution, sonicated and washed with EtOH/CH_2Cl_2/H_2O and dried under vacuum for reuse. The mixture was washed with a solution of KF (1M, 2 × 10 mL). The organic phase was extracted with AcOEt and dried with anhydrous Na_2SO_4. The solvent was removed under reduced pressure and the resulting product was purified by flash cromatography and recrystallization to give compounds **14-19**.

General procedure for CuAAC + Suzuki MMCRs (synthesis of compounds 20–25). In a coated Kimble vial containing the 3D-SiO_2-APTS-Cu (overall Cu content on monolith: 0.6 mg) and 3D-SiO_2-AAPTS-Pd (overall Pd content on monolith: 1.6 mg) monolithic catalysts, sodium azide (0.5 mmol), CsF (0.6 mmol), the corresponding iodobenzyl bromide (0.5 mmol), DIPEA (2.5 mmol), the corresponding alkyne (0.5 mmol) and the boronic acid (0.55 mmol) were dissolved in a mixture of tBuOH (4 mL) H_2O (1 mL). The mixture was heated at 90 ºC for 12 h. The mixture was allowed to cool. The solid formed on the vessel wall was dissolved in AcOEt. The monolithic catalysts were then removed from the solution, sonicated and washed with EtOH/CH_2Cl_2/H_2O and dried under vacuum for reuse. Final products were isolated by extraction with AcOEt/H_2O. The organic phase was dried with anhydrous Na_2SO_4, the solvent was removed under reduced pressure and the resulting product was purified by flash cromatography to give compounds **20**–**25**.

RESULTS AND DISCUSSION

Design, preparation and characterization of the catalysts. The design of the catalysts described here followed an overall strategy based on the achievement of a thin catalytic layer deposited on a monolithic silica support. The presence of catalytic species only on the surface of the monolith is an advantage from the point of view of minimizing the cost of production. If we compare this strategy with the manufacture of composite materials, where metal species are also inside the mass of the support -and not necessarily accessible to the reagents-, the amount of metal -the most expensive component- is necessarily much larger in the case of composite materials. Consequently, in this work we have used simple and economical procedures for the preparation of these monoliths. The SiO_2-based ink was extruded to assemble 3D-periodic structures with cylindrical symmetry. SiO_2 was selected because it is a material that can be easily extruded by 3D printing. This property, along with the possibility of sintering the printed structures at high temperature, provided monoliths with suitable mechanical strength and specific surface for applications in successive reaction cycles. Furthermore, SiO_2 has excellent reactivity for silanization, which enables easy functionalization of the surface, as discussed previously. An optimized ink based on 2-propanol and organic polymer binders was used to synthesize the printable SiO_2 support. The printability of the ink was controlled by adjusting the rheological properties and the processing conditions. The printed structures had a cylindrical woodpile design with an optimal geometry adapted to the dimensions of the Kimble vials in which the reactions were carried out (Figures 1e,i). The SiO_2 ink was extruded through nozzles with diameters of 410 μm and patterned layer by layer. The layers were formed by parallel rods of the extruded material separated by 1 mm and each layer was rotated by 90º. The final result was a structure with orthogonally interconnected rods. An as-prepared 3D SiO_2 structure with 40 layers is shown in Figure 1a.

A robust and reusable heterogeneous catalyst needs to have chemical stability and sufficient mechanical strength to resist the continuous contact with the reactor. In order to produce a structure with these properties, the printed structures were dried and calcined at high temperature (1500 ºC). During this process, the polymers and solvents were removed and the structure was sintered. The result is an interconnected structure of SiO_2 with suitable mechanical strength for numerous catalytic reactions. The XRD pattern (JCPDS 89–3434) of the calcined structure at 1500 ºC (Figure 1d) contained the peaks of the crystalline cristobalite phase of SiO_2. The SEM images (Figure 1b,c) show the microstructure of the sintered SiO_2 support. These images reveal the interconnected pores with a homogeneous periodicity and without defects or cracks. These images also show that the sintered support exhibited volumetric shrinkage, resulting in a rod diameter of 307 μm and inter-rod spacing of 607 μm, which correspond to an open porosity of ~ 50%.

In order to maximize the silanization process the monolith surface was activated by following the protocol described above. The use of silanes with three alkoxy groups is the most common starting point for substrate modification. These materials tend to be deposited as polymeric films and this gives total coverage and maximizes the introduction of organic functionality. Silica forms stable condensation products with silanes and the silane effectiveness is optimal on silica substrates. In order to immobilize copper and palladium species on the surface of the monolith we used two known and well-established silanes that contain coordinating amino groups, namely (3-aminopropyl)trimethoxysilane (APTS)[38–41] and [3-(2-aminoethylamino)propyl] trimethoxysilane (AAPTS)[36,42] for the immobilization of copper and palladium species,[41,43–45] respectively. The silanization reaction between the –OH groups on the silica surface of the $Si(OMe)_3$ groups occurs readily in refluxing anhydrous toluene in 24 hours.

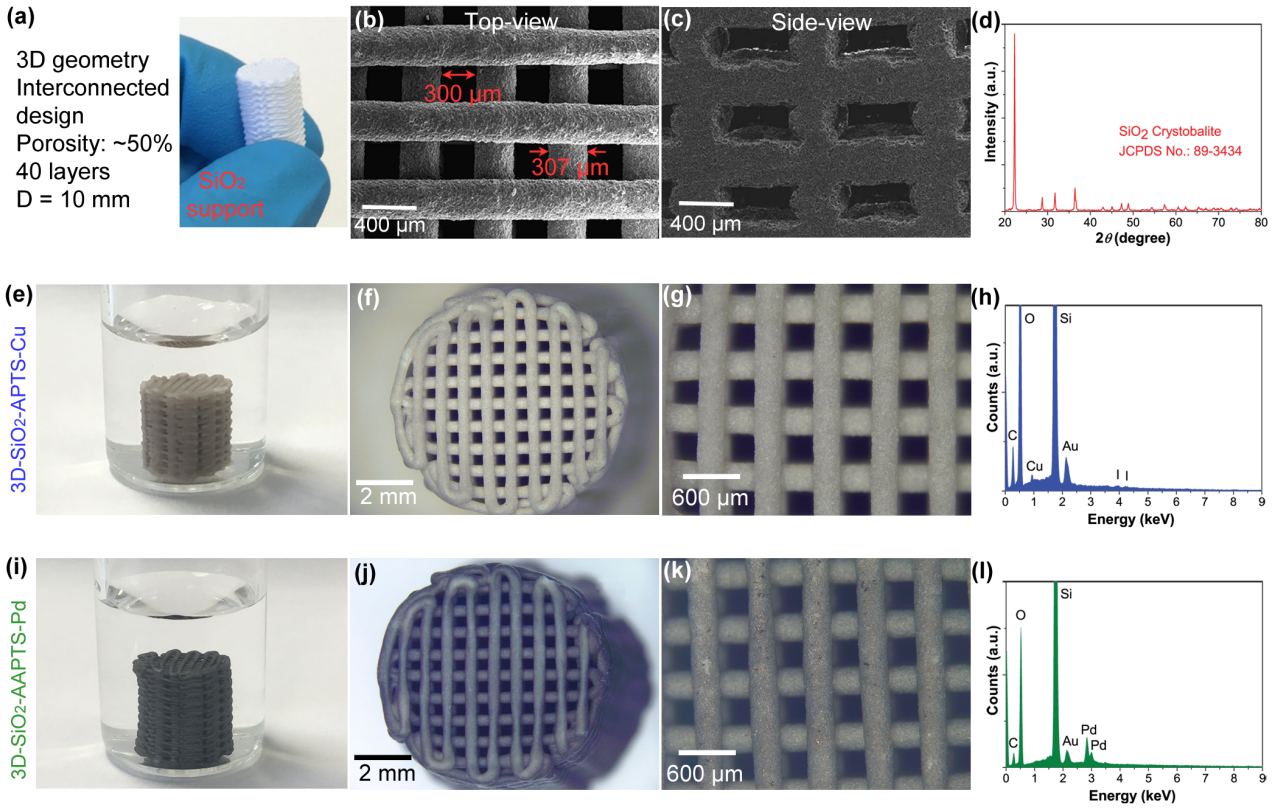

Figure 1. (a) As-prepared woodpile structure of SiO_2. SEM images of the sintered SiO_2 structure: (b) Top-view and (c) side-view, and (d) the corresponding X-ray diffraction (XRD) pattern. Optical images of the 3D-SiO_2-APTS-Cu structure: (e) in the Kimble reactor, (f) top-view, (g) high-magnification top-view, and (h) the corresponding EDS spectrum. Optical images of 3D-SiO_2-AAPTS-Pd structure: (i) in the Kimble reactor, (j) top-view, (k) high-magnification top-view, and (l) the corresponding EDS spectrum.

Once the silanizations had been carried out, the 3D printed monoliths were metallized with copper (CuI) or palladium [$Pd(AcO)_2$] species to give the target monoliths 3D-SiO_2-APTS-Cu and 3D-SiO_2-AAPTS-Pd. Optical images of the functionalized 3D-SiO_2-APTS-Cu and 3D-SiO_2-AAPTS-Pd catalysts before reaction cycles are shown in Figures 1e–g and i–k. The figures show how the color of the structures changes after the functionalization. The cream color of the 3D-SiO_2-APTS-Cu and the dark gray color of the 3D-SiO_2-AAPTS-Pd are due to the presence of Cu and Pd, respectively. The elemental composition of the structure surface was determined by Energy Dispersive Spectroscopy (EDS) analysis. These results unequivocally confirmed the presence of Cu (Figure 1h) and Pd (Figure 1l) in the respective samples. The Si and O peaks correspond to the SiO_2 substrate and the C peak corresponds to the carbon chain of the silane compound. In addition, the EDS spectrum shows the presence of an escape peak at 0.020 keV obtained with the Si(Li) EDS detector. The presence of a gold peak in both samples is due to the conductive surface sputtered onto the sample to avoid charging effects during measurement.

The copper and palladium loadings on the monolith surfaces were determined by inductively coupled plasma-optical emission spectroscopy (ICP-OES) and the values were 1.6 mg of Pd on the 3D-SiO_2-AAPTS-Pd monolith and 0.6 mg of Cu on the 3D-SiO_2-APTS-Cu monolith (average for 10 monolithic samples). All of the Pd and Cu contents are exclusively on the surface of the monolith (BET area for both monoliths: 0.3 m^2/g) thus representing the amount of catalytically available metal for the catalytic processes. This represents a percentage of 2 mol% of Cu and 3 mol% of Pd present in each catalytic reaction.

XPS experiments (Figure 2) were carried out to determine the oxidation state of palladium and copper. According to the literature, curve fitting of the Cu $2p_{3/2}$ region shows two different copper species with binding energies (BE) of 932.6 eV and 934.9 eV, which on the basis of their BEs are assigned to Cu_2O and/or Cu metal and CuO, respectively.[46] Pure Cu_2O, Cu metal, CuO and $Cu(OH)_2$ standards were analyzed and their BEs were found to be 932.6, 933.0, 933.5 and 934.0 eV, respectively. For the 3D-SiO_2-APTS-Cu sample, a deconvolution procedure used for the Cu $2p_{3/2}$ core level was performed (Figure 2a). A unique peak with a maximum at 932.2 eV was assigned to Cu(0/I). There was no evidence for the presence of Cu(II) species in the material. Due to the similar binding ener-

gies between Cu(I) and Cu(0), Auger electron spectroscopy was used to distinguish the copper species. Unfortunately, the Auger signal was too weak to distinguish between Cu(I) and Cu(0) oxidation states, but the presence of iodine in EDS analysis confirms the prevalence of Cu(I). For the 3D-SiO_2-AAPTS-Pd sample, the peak deconvolution and curve fitting of the Pd 3d core level region were also performed (Figure 2b). According to the literature, the set of double peaks at 335.5 and 340.8 eV are assigned to Pd(0), while the other double peaks at 336.9 and 342.2 eV belongs to the Pd(II) oxidation state.[47] Other elements (Si, N, O, C) were also detected in the survey XPS spectra in both monoliths (see supporting information).

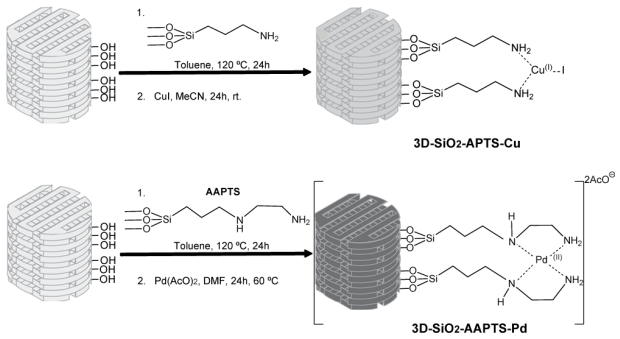

Scheme 1. Synthetic route for 3D-SiO_2-APTS-Cu and 3D-SiO_2-AAPTS-Pd. The predominant oxidation states Cu(I) and Pd(II) are showed in brackets.

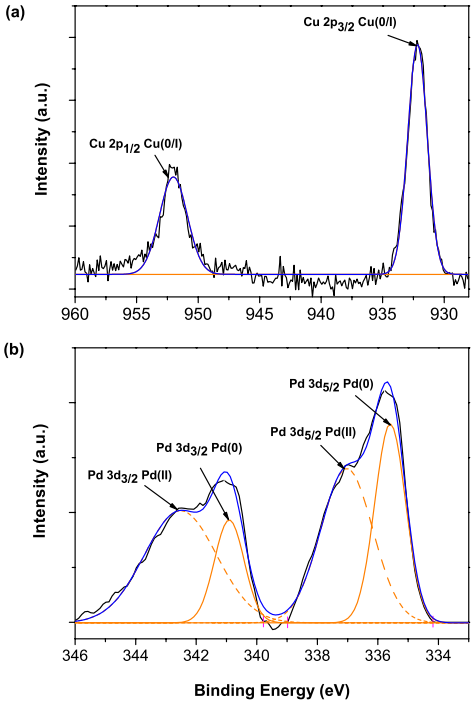

Figure 2. XPS spectra for Cu and Pd on 3D-SiO_2-APTS-Cu and 3D-SiO_2-AAPTS-Pd surfaces.

The ToF-SIMS images of the 3D-SiO_2-APTS-Cu and 3D-SiO_2-AAPTS-Pd monolith cylinder surfaces are shown in Figure 3. These images show the surface distribution of Cu, Pd, and Si on the SiO_2 monolith surface. In both 3-D catalysts, Cu and Pd were found to be present throughout the sample with a homogeneous distribution along the cylinder surface.

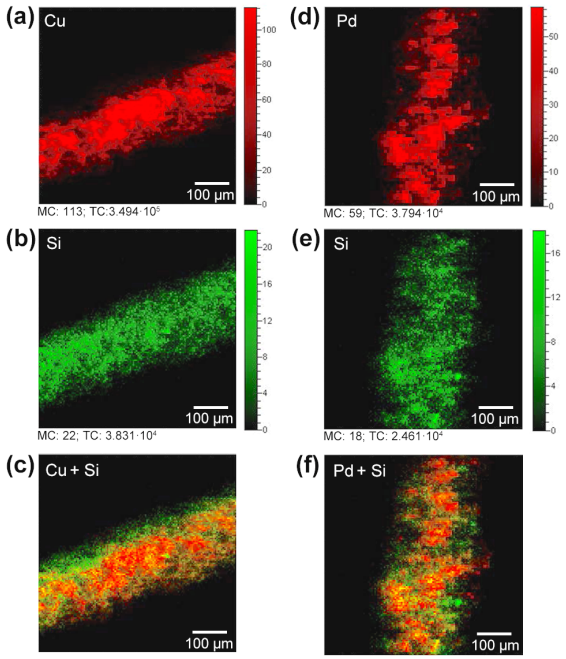

Figure 3. ToF-SIMS images showing the signal intensity of Cu and Si at SiO_2-APTS-Cu surface: (a) Cu, (b) Si, (c) Overlay of the sum of Cu and Si, and at the SiO_2-AAPTS-Pd surface: (d) Pd, (e) Si, (f) Overlay of the sum of Pd and Si. The intensities are represented on a scale with light colors indicating high intensities. MC – maximum signal (counts) per pixel. TC – total counts in the entire image. Field of view 500×500 µm².

Evaluation of the catalytic performance in MMCRs. The triazole nucleus is one of the most important and well-known heterocycles, which is a common and integral feature of a variety of natural products and medicinal agents. A large amount of research has been carried out on triazole and its derivatives and this has proved the pharmacological importance of this heterocycle.[48] The procedures developed in this work are intended to provide an efficient assembly of 1,2,3-triazoles while also allowing the expansion of chemical diversity around this ring in a rapid and efficient way by introducing different functionalities (alkenes, alkynes, aryls, heterocycles), through the use of a suitable coupling partner, at positions close to this framework. The general strategy of the catalytic process is represented in Scheme 2. In this type of transformation, four new bonds are formed during a multicomponent reaction using sodium azide, 2-, 3- or 4-iodo benzyl bromides, alkynes and a coupling partner (an organostannane reagent, boronic acid or a second molecule of alkyne). In order to connect both catalytic processes (CuAAC and PCCCR) we selected commercial 2-, 3- or 4-iodobenzyl bromides as key bifunctional reagents that are able to undergo a nucleophilic displacement of the benzylic bromo-substituent by sodium azide to form in situ the organic azide and an oxidative addition at the iodo-substituent position on the aromatic ring. The initial CuAAC between the alkyne and the in situ generated organic azide would be promoted by 3D-SiO_2-APTS-Cu while the coupling of organostannanes (Stille), boronic acids (Suzuki) or a second molecule of alkyne (Sonogashira) would be catalyzed by 3D-SiO_2-AAPTS-Pd. According to the initial design of the synthetic procedure, all of these multicatalytic processes would be developed into a one-pot version either through true MMCRs (CuAAC + Stille, CuAAC + Suzuki or CuAAC + Sonogashira 3CR) or through sequential one-pot reactions (CuAAC + Sonogashira 3+1CR,

using two different alkynes). A fundamental aspect in the MMCRs is the compatibility and stability of different unsupported reagents and solvents to carry out one-pot processes. Another challenge is the coexistence of catalytic metal species in the appropriate oxidation state to perform each catalytic process in the appropriate manner. Taking these aspects into consideration, we initially decided to optimize separately the two catalytic transformations (CuAAC and PCCCRs) using a monolith for each single reaction type in an effort to find 'consensus' conditions (optimal common base, solvent, and temperature) and finally merging the optimal conditions to give the designed MMCR.

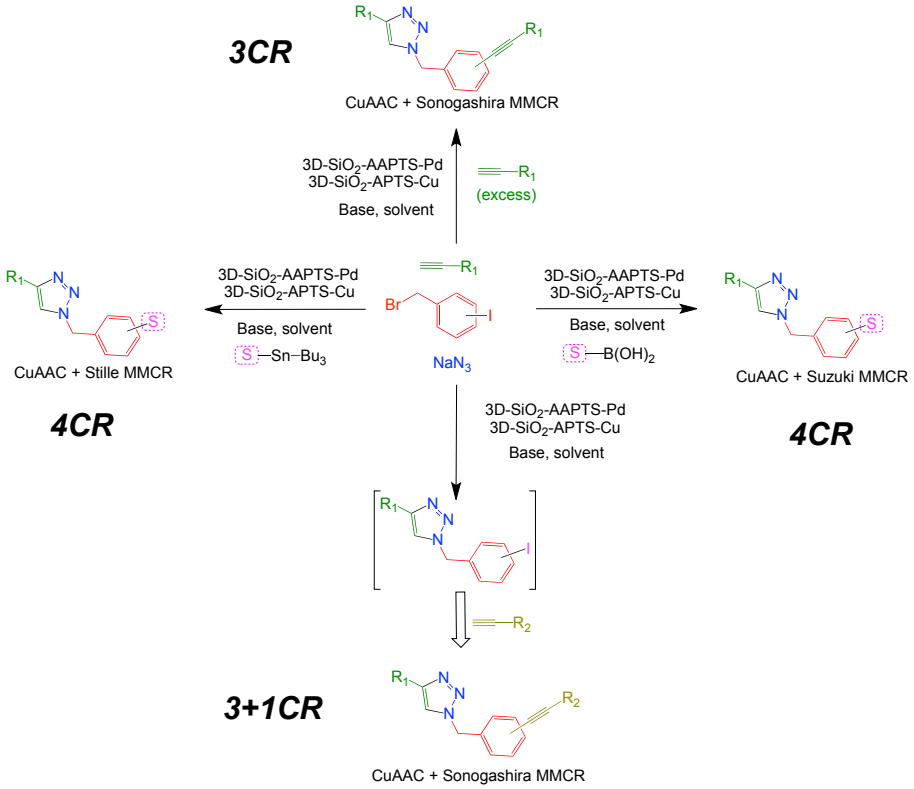

Scheme 2. General outline for the strategy of Cu-Pd MMCRs.

Catalytic optimization for single CuAAC and PCCCRs. We first tested the effectiveness of 3D-SiO_2-APTS-Cu in the three-component version of the CuAAC. We focused our efforts on obtaining optimum yields, no leaching and simple conditions using environmentally friendly solvents, such as the H_2O/tBuOH mixture. As a model test, we studied the reaction of phenylacetylene, sodium azide and 2-iodobenzyl bromide to give 1-(2-iodobenzyl)-4-phenyl-1,2,3-triazole (**1**) in the presence of a soluble base. Although the surface of the 3D-SiO_2-APTS-Cu catalyst contains basic centers due to the relatively large excess of base required for CuAAC (as well as for Sonogashira and Suzuki reactions), in order to favor the initial organic azide formation by reaction of sodium azide and 2-iodobenzyl bromide before the alkyne assembly, we envisioned that the presence of a large excess of an effective soluble base would ensure the effectiveness of the click process.[49] The results of the optimization process for CuAAC are shown in Table 1. Although the copper catalyst showed good efficiency on using different bases and solvents, to our satisfaction the use of equimolar amounts of alkyne, sodium azide and 2-iodobenzyl bromide in the presence of excess (3 equivalents) of DIPEA in tBuOH/H_2O (3:1) led the transformation to occur optimally at room temperature overnight and without the need to carry out the process in the presence of an inert atmosphere or any other reducing additive. Glaser–Eglinton homocoupling byproducts were not detected and neither was the presence of copper-promoted alkyne insertion products at the 5-position of the triazole ring or dimerization products.[49] Immediately after checking the efficiency of 3D-SiO_2-APTS-Cu in the click reaction using the latter conditions, we checked the reusability of the catalyst after washing and drying by repeating the same experiment (entry 5). The catalytic activity was virtually unchanged and an almost identical yield was obtained. The minimum amount of catalyst required for CuAAC was optimized. Smaller monoliths, containing fewer copper species on the surface resulted in poorer yields.

Table 1: Optimization for CuAAC (3CR)

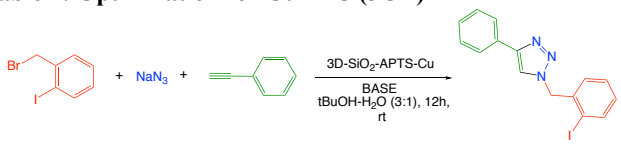

Entry	Base	Solvent	Yield (%)[a]
1	$NaHCO_3$	tBuOH/H_2O	90
2	K_2CO_3	tBuOH/H_2O	87
3	TEA	tBuOH/H_2O	92
4	DIPEA	tBuOH/H_2O	97
5	DIPEA	tBuOH/H_2O	95[b]

[a]Isolated yields. All reactions were performed using sodium azide (0.5 mmol), 2-iodobenzyl bromide (0.5 mmol), base (1.5 mmol) and phenylacetylene (0.5 mmol) a monolith 3D-SiO_2-APTS-Cu (containing 0.6 mg on surface, 2 % mol Cu), in a mixture of tBuOH (3 mL)/H_2O (1 mL). [b]Isolated yield with reused 3D-SiO_2-APTS-Cu.

Having optimized the conditions for the CuAAC, we proceeded to test the effectiveness of 3D-SiO_2-AAPTS-Pd in Sonogashira, Stille and Suzuki PCCRs. An excess of base (3 equivalents) was used in order to guarantee basic conditions for efficient Sonogashira and Suzuki transformations. Firstly, we evaluated the catalytic activity of 3D-SiO_2-AAPTS-Pd in the Sonogashira reaction without the presence of a copper co-catalyst. As proof of concept we chose triazole **1** and phenylacetylene as the starting materials while changing the base, solvent and temperature. As can be seen from the results in Table 2, 3D-SiO_2-AAPTS-Pd was effective for the coupling of phenylacetylene under different reaction conditions, although high temperatures were necessary to perform the coupling. TEA and particulary DIPEA worked well in solvents such as DMF or the tBuOH/H_2O (3:1) mixture. Once again, as in the optimization process for the catalytic performance of 3D-SiO_2-APTS-Cu in CuAAC, we evaluated the reusability of 3D-SiO_2-AAPTS-Pd (entry 6) in a second run. Changes in the catalytic behavior were not observed after two or three cycles and significant leaching (<0.1% Pd) was not detected in these studies.

Table 2: Optimization for PCCCR (Sonogashira, Stille and Suzuki reactions)

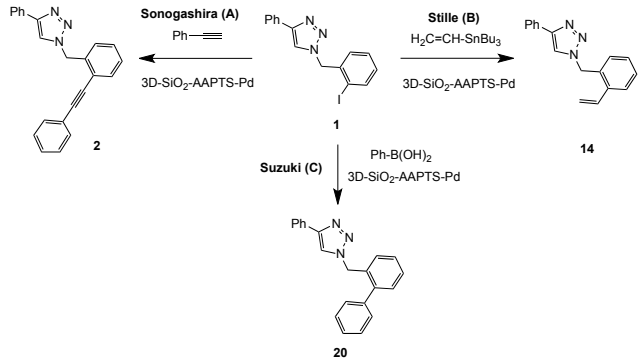

Entry	Compound /Method/Base	Solvent	Yield (%)[a]
1	**2**/A/TEA	DMF	85[b]
2	**2**/A/DIPEA	DMF	87[b]
3	**2**/A/K_2CO_3	tBuOH/H_2O	70[b]
4	**2**/A/TEA	tBuOH/H_2O	88[b]
5	**2**/A/DIPEA	tBuOH/H_2O	90[b]
6	**2**/A/DIPEA	tBuOH/H_2O	88[b,c]
7	**14**/B	Toluene	95[d]
8	**14**/B	tBuOH/H_2O	92[d]
9	**14**/B	tBuOH/H_2O	90[c,d]
10	**20**/C/K_2CO_3	Toluene/H_2O	94[e]
11	**20**/C/K_2CO_3	tBuOH/H_2O	98[e]
12	**20**/C/DIPEA	tBuOH/H_2O	99[e]
13	**20**/C/DIPEA	tBuOH/H_2O	99[c,e]

[a]Isolated yields. [b]100 ºC, 6 h. [c]Yield with reused 3D-SiO_2-APTS-Pd. [d]80 ºC, 2 h. [e]90 ºC, 2 h.

The Stille reaction is less highly valued in terms of the development of sustainable chemistry because of the inherent toxicity of tin. Despite this, due to the relative mechanistic simplicity, the stability and functional group tolerance of stannanes and its chemoselectivity, we explored the behavior of the 3D-SiO_2-AAPTS-Pd in the presence of an organostannane and the iodotriazole **1**, using the solvent mixture (tBuOH/H_2O) that was compatible with CuAAC. It can be seen from the results in Table 2 that the reactivity of 3D-SiO_2-AAPTS-Pd is excellent in organic solvents such as toluene or on using the tBuOH/H_2O (3:1) solvent mixture (entry 8). The reusability was immediately checked in a second test and changes in the reaction performance were not observed (entry 9). Finally, we checked the catalytic efficiency of 3D-SiO_2-AAPTS-Pd in the Suzuki PdCCCR using phenylboronic acid as a standard reagent in conjunction with different bases and solvents. Excellent results were obtained both in the presence of inorganic (K_2CO_3) and organic bases, particulary with DIPEA in combination with tBuOH/H_2O (1:1) for the Suzuki coupling, which gave outstanding results (Table 2). As in the case of 3D-SiO_2-APTS-Cu, smaller monoliths, containing less Pd on the surface, gave worse results, so that the concentration of catalytic species on surface is optimized using the conditions of table 2.

Catalytic activty of 3D-SiO_2-APTS-Cu and 3D-SiO_2-AAPTS-Pd in (CuAAC + PCCRs) MMCRs. Once the efficiency of 3D-SiO_2-APTS-Cu and 3D-SiO_2-AAPTS-Pd monolithic catalysts in single catalytic transformations (CuAAC or PCCRs) had been verified, we merged those optimized conditions in new MMCRs, using both catalytic monoliths simultaneously in a cooperative manner.

CuAAC + Sonogashira MMCRs. The possibility of carrying out a click reaction in conjunction with a Sonogashira coupling of a second alkyne molecule at the iodinated position of the benzyl group of the triazole in the presence of both monoliths was explored. On using equimolar amounts of sodium azide and iodobenzyl bromides, 3 equivalents of DIPEA and an excess (2.5 equivalents) of alkyne in tBuOH/H_2O (3:1), in the presence of the 3D-SiO_2-APTS-Cu and 3D-SiO_2-AAPTS-Pd monolithic catalysts, most of the transformations occurred satisfactorily within 6-12 hours (Table 3). Interestingly, when 2-iodobenzyl bromide was used in this tandem transformation under our reaction conditions there was no evidence for the formation of triazolo[5,1-*a*]isoindoles –as reported by Corma and co-workers– using Pd-Cu MOFs.[50] This finding means that the cycloaddition to generate the corresponding iodotrizole-intermediates is a favored process. In contrast, a possible intramolecular cycloaddition promoted by an initial insertion of an alkyne on the benzenic ring (promoted by Pd catalysis when using 2-iodobenzylbromide), and benzylic azide is not favored.

Table 3: CuAAC + Sonogashira MMCR (3CR)

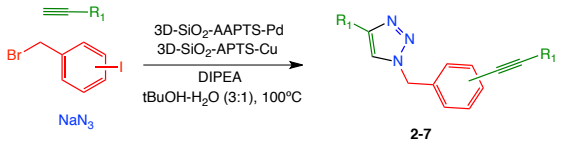

Compound	Alkyne	Halide	Yield (%)[a]
2	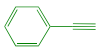	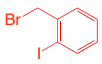	87 [b]
3	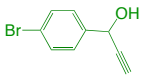	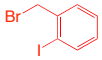	85[b]
4		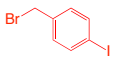	79 [c]
5		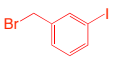	87 [b]
6	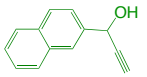	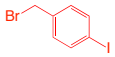	81 [b]
7	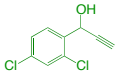	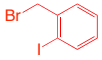	80 [b]

[a]Isolated yields. All reactions were performed using sodium azide (0.5 mmol), corresponding iodobenzyl bromide (0.5 mmol), DIPEA (1.5 mmol) and alkyne (1.2 mmol), a monolith 3D-SiO_2-APTS-Cu (containing 0.6 mg on surface, 2 % mol Cu), a 3D-SiO_2-AAPTS-Pd monolith (containing 1.6 mg on surface, 3 % mol Pd), in a mixture of tBuOH (3 mL)/H_2O (1 mL). [b]Isolated yield with reused 3D-SiO_2-APTS-Cu. [b]Reaction completed after 6 h. [c]Reaction completed after 12 h.

CuAAC + Sonogashira (one-pot sequential-3+1CR). Great structural richness can be brought about by the incorporation of diversity by two different alkynes on the triazole and on the aromatic ring of the benzyl moiety. As a consequence, the coupling of a different second alkyne molecule at the iodinated position was studied by suitable control of the reaction conditions. In order to avoid competition between alkynes in the first process (CuAAC), the strategy involved monitoring the initial click reaction in the presence of 1 equivalent of the first alkyne, and once the iodinated intermediate 1,2,3-triazole had been assembled, the addition of an excess of a second alkyne would provide the final products (Table 4). The formation of the 1,2,3-iodo-triazole intermediates occurs in a few hours in the presence of both catalysts 3D-SiO_2-APTS-Cu and 3D-SiO_2-AAPTS-Pd at room temperature. Thus, the simple addition of an excess of a second alkyne generates the final products in satisfactory yields and only traces of the CuAAC + Sonogashira MMCR compounds generated exclusively by the first alkyne were detected.

Table 4: CuAAC + Sonogashira (sequential-3+1CR)

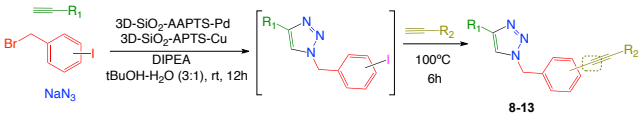

Compound	Alkyne1	Halide	Alkyne2	Yield (%)[a]
8			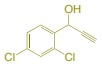	85
9			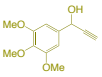	87
10				82
11				83
12				80
13				82

[a]Isolated yields after purification. All reactions were performed using sodium azide (0.5 mmol), corresponding iodobenzyl bromide (0.5 mmol), DIPEA (1.5 mmol) and first alkyne (0.5 mmol), a 3D-SiO_2-APTS-Cu monolith (containing 0.6 mg on surface, 2 % mol Cu), a 3D-SiO_2-AAPTS-Pd monolith (containing 1.6 mg on surface, 3 % mol Pd), in a mixture of tBuOH (3 mL)/H_2O (1 mL). Iodo-intermediates not isolated. TLC monitoring after 12 h confirmed completion of the first step (CuAAC) for all samples, before addition of the second alkyne (0.6 mmol).

CuAAC + Stille MMCRs. The combined use of 3D-SiO_2-APTS-Cu and 3D-SiO_2-AAPTS-Pd catalysts in Cu-AAC + Stille MMCRs was studied using different organostannanes as the coupling partner and the previously optimized base/solvent/temperature system (DIPEA/tBuOH-H_2O/80 ºC). Interestingly, under these reaction conditions only traces of a second alkyne insertion on the iodinated position of the benzenic ring were detected. Therefore, the Pd cross-coupling reaction on the iodinated position of the benzyl ring is almost exclusively generated by the organostannane-mediated transmetallation. The reaction products were formed in excellent yields (Table 5) and in many cases, after cooling the reaction mixture, the final product crystallized on the walls of the vial (Figure 4b). These reaction conditions were used to couple vinyl, ethoxyvinyl or 4-pyridyl fragments to the benzyl ring with satisfactory yields and significant differences were not found in reactivity on using different benzyl iodides in the presence of alkynes such as phenylacetylene or propynols. These results demonstrate not only the effectiveness of the combined use of the two monoliths for this type of transformation but also the compatibility of organostannanes in this type of catalytic cocktail.

CuAAC + Suzuki MMCRs. Boronic acids are in many aspects ideal partners in the CuAAC reaction methodology. The organoboron derivatives employed frequently exhibit air and water stability at ambient temperature, show little toxicity when compared to other ubiquitous organometallics and allow a range of other synthetic manipulations to be performed in their presence. Copper is known to be insert to the carbon–boron bond, which leads to useful coupling reactions when desired.[46,51] In practice, boronic acids have very different stabilities in the presence of Cu(I) and Cu(II).

Table 5: CuAAC + Stille MMCR (4CR)

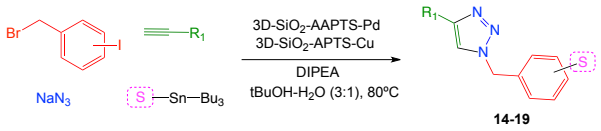

14-19

Compound	Alkyne	Halide	S	Yield (%)[a]
14				88
15				85
16				87
17				88
18				87
19				88

[a]Isolated yields. Reaction completed after 12 h. All reactions were performed using sodium azide (0.5 mmol), the corresponding iodobenzyl bromide (0.5 mmol), DIPEA (1.5 mmol), the alkyne (0.5 mmol), the organostannane (0.55 mmol), a 3D-SiO_2-APTS-Cu monolith (containing 0.6 mg on surface, 2 % mol Cu) and a 3D-SiO_2-AAPTS-Pd monolith (containing 1.6 mg on surface, 3 % mol Pd), in a mixture of tBuOH (3 mL)/H_2O (1 mL), 12h.

Encouraged by the success of the previous MMCRs using both catalysts simultaneously in a cooperative manner, we initially studied the catalytic behavior of our system following a CuAAC + Suzuki strategy using 3D-SiO_2-APTS-Cu and 3D-SiO_2-AAPTS-Pd in a new MMCR by mixing a boronic acid, sodium azide, the corresponding alkyne, the iodobenzyl bromide, and the DIPEA/tBuOH-H_2O system at 90 °C. Unfortunately, these conditions led to different degrees of degradation of the boronic acid (probably due to the insertion of Cu at the boron center). Consequently, the yields of this reaction were low on using these initial conditions, with the iodinated intermediate obtained to a large extent. In order to overcome these drawbacks to perform the classical CuAAC without interference from the reactivity between boronic acids and azide, we used CsF (which protects boronic acid in the copper(I)-mediated click reaction)[52] as a key component in the multicomponent mixture in order to protect boron from copper coordination. Under these conditions, the reaction products were obtained in satisfactory yields and with the presence of only traces of side products (Table 6). Furthermore, the absence of Chan–Lam coupling by-products (aryl azides)[51] demonstrates that Cu(II) catalysis is not operating under our reaction conditions. The application of the multicomponent strategy involving boronic acids (CuAAC + Suzuki) or organostannanes (CuAAC + Stille) in the cocktail represents a saving of several synthetic steps with respect to previous procedures for the preparation of this kind of bis-aryl triazole.[53]

Table 6: CuAAC + Suzuki MMCR (4CR)

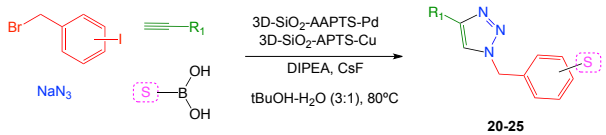

20-25

Compound	Alkyne	Halide	S	Yield (%)[a]
20				85
21				78
22				80
23				82
24				85
25				79

[a]Isolated yield. Reaction completed after 12 h. All reactions were performed using sodium azide (0.5 mmol), CsF (0.6 mmol), the corresponding iodobenzyl bromide (0.5 mmol), DIPEA (2.5 mmol), the corresponding alkyne (0.5 mmol), the boronic acid (0.55 mmol), a 3D-SiO_2-APTS-Cu monolith (containing 0.6 mg on surface, 2 % mol Cu) and a 3D-SiO_2-AAPTS-Pd monolith (containing 1.6 mg on surface, 3 % mol Pd), in a mixture of tBuOH (3 mL)/H_2O (1 mL), 12h.

Reusability, leaching studies, and characterization after catalytic performance. Recycling studies were carried out using the general procedures for single CuAAC (3D-SiO_2-APTS-Cu), Sonogashira, Stille and Suzuki (3D-SiO_2-AAPTS-Pd) transformations. After completing the reactions, each monolithic catalyst was easily removed from the reaction mixture. Both catalysts were exhaustively washed and sonicated with EtOH, CH_2Cl_2, and H_2O to remove residual salts and organics from the surface. Prior to reuse, the catalysts were dried under vacuum at room temperature. The results of the recycling process are provided in Figure 4c. As can be seen, although some changes in the oxidation state were detected for both catalysts after several runs (Figure 4d–f), both of them could be recycled and reused at least 10 times in all types of single transformations mentioned above without a noticeable drop in the product yields or catalytic activity. In the same way, when MMCRs were performed, the Pd or Cu catalysts could be reused separately in new reaction cycles.

Heterogeneous catalysts often suffer extensive leaching of the active metal species during reactions and eventually lose their catalytic activity. Another problematic issue is the case of fast back-redeposition of soluble species on the support. To determine these aspects, and if our copper and palladium monolithic catalysts operate through true heterogeneous catalysis, we performed complementary experiments at two levels. Firstly, elemental analysis (ICP) of the filtrate after the reaction demonstrated that leaching of Cu (in CuAAC) or Pd (in Sonogashira, Stille or Suzuki reactions) is negligible. In all cases, less than 1 ppm of Pd and Cu was present in the solutions at the end of the reactions, corresponding to a loss of only 0.07% (for 3D-SiO_2-APTS-Cu) and 0.03% (for 3D-SiO_2-AAPTS-Pd) of the initially added catalyst. Final content on organic products were also measured by ICP, showing 0.01

ppm of Cu for compound **1** and 0.09 ppm of Pd for compound **20**. Secondly, two key experiments (a hot filtration test and three phase tests) were carried out to evaluate whether the leached metal species are responsible for the catalytic activity. These methods are simple and powerful ways to identify when the starting solid catalytic material is a reservoir of active soluble palladium species (i.e., the filtrate conserving the same activity).

Hot filtration tests. Two couples of twin experiments were carried out for both model CuAAC and PCCCRs. In the first case, the synthesis of compound **1** was studied using sodium azide, 2-iodobenzyl bromide, and phenylacetylene, using DIPEA and tBuOH/H_2O, at room temperature in the presence of 3D-SiO_2-APTS-Cu (same conditions of table 1, entry 4). After 6 hours (50% conversion), 3D-SiO_2-APTS-Cu was removed from the vial. The CuAAC course in the filtrate was followed by TLC and compared with the twin experiment in which the catalyst was maintained. In the same manner, for the study of a possible leaching of 3D-SiO_2-AAPTS-Pd in a model PCCCR, we first analyzed the synthesis of compound **20** by Suzuki reaction using the iodotriazole **1**, phenylboronic acid, DIPEA in tBuOH/H_2O (same conditions of table 2, entry 12) performing two twin experiments as before, and removing the catalyst in one of the experiments after 50% of the transformation (TLC control). As a common result for both transformations, in the filtrates, the formation of both final products (**1** for CuAAC, **20** for Suzuki reaction) did not proceed further. These filtering experiments indicated that with these monolithic catalysts we are dealing with heterogeneous catalytic systems.

Three Phase Tests. In the case of 3D-SiO_2-APTS-Cu monolith, the three-phase test was carried out in analogy to the procedure published by our group.[54] A couple of experiments using a supported azide demonstrated no leaching of copper from the monolith (see supporting information). For 3D-SiO_2-AAPTS-Pd: we followed the synthesis presented by Crudden et al. [55,56] (for detailed procedures, see supporting information). Silica supported 4-Bromo-benzamide 3-propyltriethoxy-silane was prepared. A model Suzuki reaction was performed. To ensure that an active catalyst is present, a soluble aryl halide, i.e., 4-bromoacetophenone, is added. After reaction, the soluble portion was analyzed after filtration while the amide is hydrolyzed from the support and isolated as carboxylic acid. 1-([1,1'-biphenyl]-4-yl)ethanone was isolated. But [1,1'-biphenyl]-4-carboxylic acid formation was not detected. It demostates apparent no leaching of Pd from our monolith.

Catalyst characterization after catalysis. The SEM images did not show significant changes in the monolithic surface morphology of 3D-SiO_2-APTS-Cu and 3D-SiO_2-AAPTS-Pd after carrying out the different catalytic reactions. This reflects their good stability after reuse (see Figure S2, supporting information).

A slight change in color (from slightly brown to slightly greenish) was often observed in 3D-SiO_2-APTS-Cu and 3D-SiO_2-AAPTS-Pd turned even darker after 10 cycles. In order to determine whether during the reaction cycles a progressive change occurs in the oxidation state of surface metal species, XPS analysis of different samples after catalysis were performed. The studies performed on 3D-SiO_2-APTS-Cu indicated a slight oxidation of copper present on surface. A small deconvoluted peak of Cu(II) (35% content) is observed at 933.5 eV (Figure 4d). However, a total reactivation of the oxidation state (0/I) in 3D-SiO_2-APTS-Cu catalyst can be carried out by treatment of the reused catalyst with an aqueous solution of sodium ascorbate (2M) for 3 h (Figure 4e). In the case of the palladium catalyst, XPS spectra performed in different samples indicated that during the different reaction cycles, the 3D-SiO_2-AAPTS-Pd catalyst presented a high conversion of the initially existing Pd(II) fraction to Pd(0). However, this reduction process of the palladium does not affect the catalytic activity (see Figure 4f).

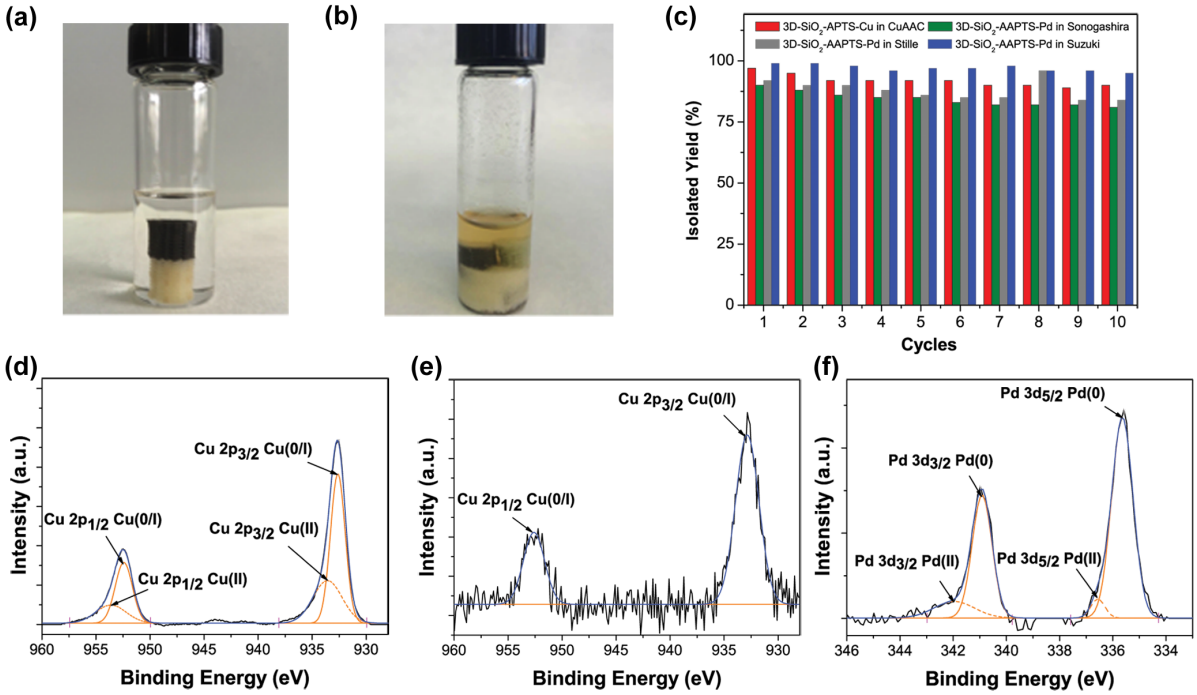

Figure 4. Photographs showing a Kimble vial in a typical CuAAC + Stille MMCR experiment (compound 14) using 3D-SiO_2-APTS-Cu and 3D-SiO_2-AAPTS-Pd in tBuOH/H_2O (a) before addition of the starting materials and carrying out the reaction (b) after the CuAAC + Stille MMCR. (c) Reusability of 3D-SiO_2-APTS-Cu and 3D-SiO_2-AAPTS-Pd. (d) XPS spectra of the Cu on 3D-SiO_2-APTS-Cu after catalytic reactions. (e) after treatment with sodium ascorbate and (f) XPS spectra of Pd on 3D-SiO_2-AAPTS-Pd after catalytic reactions (10 cycles).

CONCLUSIONS

Recently, the relationships between catalyst structures and catalytic performance have received a great deal of attention. Modulation of these aspects can be performed by 3D printing, an emerging technology that enables the fabrication of complex 3D catalysts in a more efficient way compared with traditional manufacturing processes. In this work, we have demonstrated that a combination of 3D printing of silica monoliths and an appropriate surface modification on the silica support (i.e., silanization and metallation) is an excellent approach for the fabrication of new, efficient, robust and easy reusable monolithic Pd- and Cu-based catalysts to perform MMCRs. Since these heterogeneous catalysts are stable – they show negligible metal leaching – they can be reused more than 10 times. In addition, compartmentalization of Pd and Cu species in these monoliths allows individual recycling after performing each kind of MMCR. The catalytic effectiveness and ease of handing of these monolithic prototypes in work up processes make these devices very suitable for solution phase chemistry in industrial applications.

ASSOCIATED CONTENT

Supporting Information

(The Supporting Information is available free of charge on the ACS Publications website at DOI: ----------).
Detailed experimental procedures, supporting figures and tables (PDF)

AUTHOR INFORMATION

Corresponding Author

*A.C. albertojose.coelho@usc.es

*A.G. alvaro.gil@usc.es

Author Contributions

‡Antonio S. Díaz-Marta and Carmen R. Tubío contributed equally. The manuscript was written through contributions of all authors. All authors have given approval to the final version of the manuscript.

Notes

The authors declare no competing financial interest.

ACKNOWLEDGMENT

This work received financial support from the Xunta de Galicia (EM2014/022 to A. Coelho, ED431B2016/028 to F. Guitián and ED431B2017/70 to E. Sotelo). The work was also funded by the Consellería de Cultura, Educación e Ordenación Universitaria (Centro singular de investigación de Galicia accreditation 2016-2019, ED431G/09) and the European Regional Development Fund (ERDF).

REFERENCES

(1) Anastas, P. T.; Warner, J. C. In *Green chemistry: theory and practice*; Oxford University Press: New York, 1998; p 30.
(2) Petrone, D. A.; Ye, J.; Lautens, M. *Chem. Rev.* **2016**, *116*, 8003–8104.
(3) Crawley, M. L.; Trost, B. M. In *Applications of Transition Metal Catalysis in Drug Discovery and Development: An Industrial Perspective*; John Wiley & Sons, 2012; p 13.
(4) Ciriminna R., Cará P. D., Sciortino M., Pagliaro M. *Adv. Synth. Catal.* **2011**, *353*, 677–687.
(5) Millini, R.; Bellussi, G. *Catal. Sci. Technol.* **2016**, *6*, 2502–2527.
(6) Zhou, H.-C. "Joe"; Kitagawa, S. *Chem. Soc. Rev.* **2014**, *43*, 5415–5418.
(7) Gascon, J.; Corma, A.; Kapteijn, F.; Llabrés i Xamena, F. X. *ACS Catal.* **2014**, *4*, 361–378.
(8) Parvulescu, V. I.; Kemnitz, E. In *New Materials for Catalytic Applications*; Elsevier, 2016; p 13.
(9) Díaz, U.; Brunel, D.; Corma, A. *Chem. Soc. Rev.* **2013**, *42*, 4083–4097.
(10) Kolb, H. C.; Finn, M. G.; Sharpless, K. B. *Angew. Chem. Int. Ed Engl.* **2001**, *40*, 2004–2021.
(11) Liang, L.; Astruc, D. *Coord. Chem. Rev.* **2011**, *255*, 2933–2945.
(12) Rostovtsev, V. V.; Green, L. G.; Fokin, V. V.; Sharpless, K. B. *Angew. Chem. Int. Ed Engl.* **2002**, *41*, 2596–2599.
(13) Tornøe, C. W.; Christensen, C.; Meldal, M. *J. Org. Chem.* **2002**, *67*, 3057–3064.
(14) Johansson Seechurn, C. C.; Kitching, M. O.; Colacot, T. J.; Snieckus, V. *Angew. Chem. Int. Ed Engl.* **2012**, *51*, 5062–5085.
(15) Pagliaro, M.; Pandarus, V.; Ciriminna, R.; Béland, F.; Demma Carà, P. *ChemCatChem* **2012**, *4*, 432–445.
(16) Herrera, R. P.; Marqués-López, E. In *Multicomponent Reactions: Concepts and Applications for Design and Synthesis*; John Wiley & Sons, 2015; p 1.
(17) Cioc, R. C.; Ruijter, E.; Orru, R. V. A. *Green Chem.* **2014**, *16*, 2958.
(18) Climent, M. J.; Corma, A.; Iborra, S. *RSC Adv.* **2012**, *2*, 16–58.
(19) Galván, A.; Fañanás, F. J.; Rodríguez, F. *Eur. J. Inorg. Chem.* **2016**, *9*, 1306–1313.
(20) Lebel, H.; Ladjel, C.; Bréthous, L. *J. Am. Chem. Soc.* **2007**, *129*, 13321–13326.
(21) Gu, S.; Xu, D.; Chen, W. *Dalton Trans.* **2011**, *40*, 1576–1583.
(22) Tsoung, J.; Panteleev, J.; Tesch, M.; Lautens, M. *Org. Lett.* **2014**, *16*, 110–113.
(23) Zhang, L.; Sonaglia, L.; Stacey, J.; Lautens, M. *Org. Lett.* **2013**, *15*, 2128–2131.
(24) Qiu, G.; Ding, Q.; Ren, H.; Peng, Y.; Wu, J. *Org. Lett.* **2010**, *12*, 3975–3977.
(25) Lee, D. J.; Han, H. S.; Shin, J.; Yoo, E. J. *J. Am. Chem. Soc.* **2014**, *136*, 11606–11609.
(26) Ramos-Fernandez, E. V.; Garcia-Domingos, M.; Juan-Alcañiz, J.; Gascon, J.; Kapteijn, F. *Appl. Catal. Gen.* **2011**, *391*, 261–267.
(27) Liu, J.; Sun, W. In *Magnetic Nanomaterials: Applications in Catalysis and Life Sciences;* The Royal Society of Chemistry: UK, 2017; p 59–98.
(28) Phan, N. T. S.; Gill, C. S.; Nguyen, J. V.; Zhang, Z. J.; Jones, C. W. *Angew. Chem. Int. Ed.* **2006**, *45*, 2209–2212.
(29) Houghten, R. A. *Proc. Natl. Acad. Sci. U. S. A.* **1985**, *82*, 5131–5135.
(30) Yashnik, S. A.; Denisov, S. P.; Danchenko, N. M.; Ismagilov, Z. R. *Appl. Catal. B Environ.* **2016**, *185*, 322–336.
(31) Corma, A. *Angew. Chem. Int. Ed.* **2016**, *55*, 6112–6113.
(32) Lewis, J. A.; Smay, J. E.; Stuecker, J.; Cesarano III, J. *J. Am. Ceram. Soc.* **2006**, *89*, 3599–3609.
(33) Zhou, X.; Liu, C. *Adv. Funct. Mater.* **2017**, *27*, 1701134.
(34) Wang, X.; Guo, Q.; Cai, X.; Zhou, S.; Kobe, B.; Yang, J. *ACS Appl. Mater. Interfaces* **2014**, *6*, 2583–2587.
(35) Tubío, C. R.; Azuaje, J.; Escalante, L.; Coelho, A.; Guitián, F.; Sotelo, E.; Gil, A. *J. Catal.* **2016**, *334*, 110–115.
(36) Zhu, M.; Lerum, M. Z.; Chen, W. *Langmuir ACS J. Surf. Colloids* **2012**, *28*, 416–423.
(37) Lu, X.; Lee, Y.; Yang, S.; Hao, Y.; Evans, J. R. G.; Parini, C. G. *J. Eur. Ceram. Soc.* **2010**, *30*, 1–10.
(38) Howarter, J. A.; Youngblood, J. P. *Langmuir ACS J. Surf. Colloids* **2006**, *22*, 11142–11147.

(39) Wang, S.; Wen, S.; Shen, M.; Guo, R.; Cao, X.; Wang, J.; Shi, X. *Int. J. Nanomedicine* **2011**, *6*, 3449–3459.
(40) Shen, M.; Cai, H.; Wang, X.; Cao, X.; Li, K.; Wang, S. H.; Guo, R.; Zheng, L.; Zhang, G.; Shi, X. *Nanotechnology* **2012**, *23*, 105601.
(41) Xiong, X.; Cai, L. *Catal. Sci. Technol.* **2013**, *3*, 1301–1307.
(42) Zhang, L.-Y.; Wang, L. *Chin. J. Chem.* **2008**, *26*, 1601–1606.
(43) Li, H.; Wang, L.; Li, P. *Synthesis* **2007**, *11*, 1635–1642.
(44) Miao, T.; Wang, L. *Synthesis* **2008**, *3*, 363–368.
(45) Jumde, R. P.; Evangelisti, C.; Mandoli, A.; Scotti, N.; Psaro, R. *J. Catal.* **2015**, *324*, 25–31.
(46) He, Z.; Lin, H.; He, P.; Yuan, Y. *J. Catal.* **2011**, *277*, 54–63.
(47) Priolkar, K. R.; Bera, P.; Sarode, P. R.; Hegde, M. S.; Emura, S.; Kumashiro, R.; Lalla, N. P. *Chem. Mater.* **2002**, *14*, 2120–2128.
(48) Kharb, R.; Sharma, P. C.; Yar, M. S. *J. Enzyme Inhib. Med. Chem.* **2011**, *26*, 1–21.
(49) Angell, Y.; Burgess, K. *Angew. Chem. Int. Ed.* **2007**, *46*, 3649–3651.
(50) Arnanz, A.; Pintado-Sierra, M.; Corma, A.; Iglesias, M.; Sánchez, F. *Adv. Synth. Catal.* **2012**, *354*, 1347–1355.
(51) Grimes, K. D.; Gupte, A.; Aldrich, C. C. *Synthesis* **2010**, *9*, 1441–1448.
(52) Jin, S.; Choudhary, G.; Cheng, Y.; Dai, C.; Li, M.; Wang, B. *Chem. Commun. Camb. Engl.* **2009**, *21*, 5251–5253.
(53) White, J. R.; Price, G. J.; Schiffers, S.; Raithby, P. R.; Plucinski, P. K.; Frost, C. G. *Tetrahedron Lett.* **2010**, *51*, 3913–3917.
(54) Coelho, A.; Diz, P.; Caamaño, O.; Sotelo, E. *Adv. Synth. Catal.* **2010**, *352*, 1179–1192.
(55) Webb, J. D.; MacQuarrie, S.; McEleney, K.; Crudden, C. M. *J. Catal.* **2007**, *252*, 97–109.
(56) Bedford, R. B.; Singh, U. G.; Walton, R. I.; Williams, R. T.; Davis, S. A. *Chem. Mater.* **2005**, *17*, 701–707.

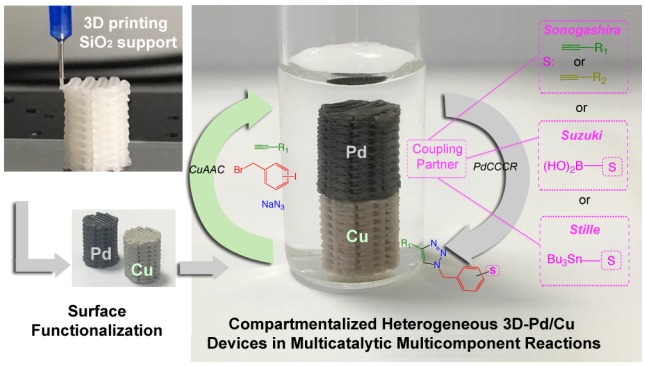
3D printing
SiO2 support
Pd
Cu
Surface
Functionalization
CuAAC
NaN3
Pd
Cu
Coupling
Partner
PdCCCR
Sonogashira
or
Suzuki
or
Stille
Compartmentalized Heterogeneous 3D-Pd/Cu
Devices in Multicatalytic Multicomponent Reactions